Piotr Śliwiński, Marek St. Węglowski, Kamil Kubik, Piotr Gotkowski

DOI: 10.32730/mswt.2024.68.2.5

Electron Beam Welding of High-Strength Aluminium Alloys

Spawanie wysokowytrzymałych stopów aluminium wiązką elektronów

Abstract: Owing to the greater precision of energy density control, the highest possible metallurgical purity of the process and the lack of sensitivity to reflectivity and surface roughness, electron beam welding is a suitable method for joining aluminium alloys. The paper presents results concerning the welding of aluminium alloy grades 6060 and 6061 as well as experimental alloys having higher copper contents. The tests discussed in the paper led to the obtainment of joints characterised by a high strength of up to 289.7 MPa and the lack of unacceptable imperfections.

Key words: welding, electron beam, aluminium, metallography, microstructures, mechanical properties

Streszczenie: Spawanie wiązką elektronów, ze względu na większą precyzję kontroli gęstości energii, najwyższą możliwą czystość metalurgiczną procesu oraz brak wrażliwości na współczynnik odbicia światła i chropowatość powierzchni, jest odpowiednią metodą łączenia stopów aluminium. W niniejszym artykule przedstawiono wyniki spawania stopów aluminium w gatunku: 6060, 6061, a także eksperymentalnych stopów o podwyższonej zawartości miedzi. W ramach badań uzyskano złącza charakteryzujące się wysoką wytrzymałością, nawet do 289,7 MPa, a także brakiem niedopuszczalnych niezgodności.

Słowa kluczowe: spawanie, wiązka elektronów, aluminium, metalografia, mikrostruktury, własności mechaniczne

1. Introduction

Aluminium is one of the most frequently used materials in the automotive, shipbuilding, railway, aviation, space and nuclear power industries. Challenges accompanying the joining of aluminium include its susceptibility to deformation, the formation of oxide layers, sensitivity to process purity, high thermal conductivity, high melting point, the toxicity of welding fume as well as susceptibility to hot cracking and porosity. Physical properties of aluminium such as high thermal conductivity, high thermal expansion coefficient, the lack discolouration at high temperatures and large differences in melting points of the metal and its oxide (~1400 °C) increase welding-related difficulties [1–5].

Arc welding methods (GTAW, GMAW, and PAW) are commonly industrially used in the joining of aluminium alloys. However, in cases of the above-named welding methods, the controllability of linear energy, density and energy distribution is limited, thus precluding the prevention of phenomena resulting from the thermal expansion of the metal, its deformations or hot cracking. In terms of some aluminium alloys, such as 6xxx series alloys, the welding process entails the use of consumables of chemical compositions different to those of elements subjected to welding, which could further worsen properties of joints. Laser beam or electron beam welding enable significantly greater precision in terms of energy density control by changing the position of the beam focus and setting the beam into oscillations of a given amplitude. Laser beam or electron beam welding processes are also (mostly) fully automated or robotic [2–5].

In addition, if a given structure contains heat-sensitive parts located near welded joints, welding processes characterised by high energy density (such as electron beam welding (EBW)) are the best when it comes to welding aluminium [2–5].

It should also be noted that the laser welding of aluminium is additionally complicated by the susceptibility of the technology to high laser light reflectivity from the surface of the material subjected to welding. In addition, laser welds are often characterised by increased porosity [2–5].

In view of the foregoing, the electron beam welding process appears to be the most suitable method for the joining of elements made of aluminium alloys.

2. Overview of reference publications

Researchers from an international team (M. Lipińska et al.) [6] performed tests involving the electron beam welding process and specimens made of variously-grained Al-Mg-Si alloys. The welding parameters were selected in a manner enabling the reduction of linear energy and, consequently, the heat affected zone (HAZ) as well as the evaporation of chemical elements characterised by high saturated vapour pressure. The ultra-fine-grained microstructure (UFG) of one of the alloys enabled the obtainment of smaller grains in the fusion zone (FZ) and heat affected zone (HAZ), which led to the higher mechanical strength of the weld than that

mgr. inż. Piotr Śliwiński, dr inż. Marek St. Węglowski, mgr inż. Kamil Kubik, mgr inż. Piotr Gotkowski – Łukasiewicz Research Network – Upper Silesian Institute of Technology, Gliwice, Poland

Corresponding Author: piotr.sliwinski@git.lukasiewicz.gov.pl

of welds made of alloys characterised by the lower degree of grain refinement (i.e. coarse-grained microstructure). The tensile strength of a joint made of the coarse-grained alloy (CG) amounted to 80 %, whereas that of the UFG specimen was 68 % (i.e. 82 % if compared with the coarse-grained base material). The reasons for the deterioration of the mechanical properties of the fusion zone (FZ) included the dissolution of precipitates hardening the alloy structure and an increase in the grain size. The process was also accompanied by the greater evaporation of Mg (alloying element) and Zn (impurity). During the tensile tests, both specimens (welds) ruptured in the fusion line.

South-Korean researchers (Soo-sung Kim et al.) [7] performed tests aimed to develop the electron beam welding process usable in the fabrication of a system of plates supporting nuclear fuel rods. The researchers performed initial tests concerning the fabrication of fuel plates, taking into account welding process efficiency when using aluminium alloy grade AA6061-T6. The tests led to the obtainment of optimum welding parameters in relation to the fuel plate unit in terms of accelerating voltage, beam current and welding time. Welds made using the optimum parameters were characterised by lower tensile strength than that of the specimens not subjected to welding. The strength of the specimens constituted 52 % of the base material strength as regards the specimens subjected to tension in transverse direction (in relation to the rolling direction) and 58 % of the base material strength as regards the specimens subjected to tension in the direction parallel to rolling.

A Greek team led by Nikolaos Alexopoulos tested [8] mechanical properties of electron beam welded specimens made of aluminium alloy 6156. Sheets made of alloy AA6156 were subjected to pre and post-weld artificial ageing (at a temperature of 170 °C), whereas specimens used in tensile tests were prepared in accordance with the ASTM E8 standard. The time of processing corresponded to various types of precipitation hardening. The test results revealed that welding not accompanied by heat treatment led to the reduction of the yield point by approximately 100 MPa, whereas elongation at rupture did not exceed 4 %. The tests also revealed that pre-weld artificial ageing increased plasticity at tension (elongation at tension increased by half), whereas post-weld artificial ageing significantly increased mechanical properties (strength constituted more than 75 % of that of the base material).

Fatih Hayat tested [9] the electron beam welding (EBW) of aluminium alloys of series 7075. The welding process was performed using two different values of welding current (i.e. 20 mA and 25 mA). The test specimens were subjected to tensile tests aimed to identify mechanical properties. Other tests included the investigation of surfaces in the area of rupture as well as microhardness tests and tests involving the use of scanning electron microscopy (SEM) and energy dispersive spectrometry-based analysis (EDS). The SEM tests included the examination of microstructural changes in welded joints in the base material (BM), heat affected zone (HAZ) and in the fusion zone (FZ). The post-weld (EBW) results revealed an increase in microhardness in the fusion zone (FZ) in comparison with that of the base material (BM) and in the heat affected zone (HAZ). The lowest hardness was observed in the HAZ. The researchers attempted to identify intermetallic compounds in the fusion zone and the effect of chemical elements on cracking. In relation to 20 mA and 25 mA, the joints made of alloy 7075 and subjected to tensile tests underwent brittle cracking. It was possible to observe an increase in the amount of Cu at the area of rupture. The aforesaid increased presence of copper triggered the cracking of the joints, particularly of that made using higher current; the joint was also characterised by lower tensile strength (i.e. 297 MPa and 256 MPa respectively).

The authors of another research work (P. Wanjarai et al.) [10] performed tests involving electron beam welded joints made of aluminium alloy AA2024. The tests revealed that, in terms of the butt welding of 5 mm thick plates, there was a threshold value of beam current, the exceeding of which led to the formation of incompletely filled grooves which failed to meet quality-related criteria. In cases of beam focusing, a change of the focal point position from the surface to a position below the bottom part of the plate indicated that weld shape regularity and quality were optimum when the beam was focused near the centre of the workpiece thickness. The tests also revealed that welding with the non-oscillating beam followed by subsequent smoothing of the bead produced more favourable results than the welding process involving the use of the oscillating beam and without subsequent smoothing. As a result, the optimum conditions during the welding of AA2024 included the beam focused at the centre of the plate thickness, the use of the non-oscillating beam, an input power of 2.5 kW and a welding rate of 34 mm/s. In relation to the above-presented conditions, the weld microstructure contained the columnar dendritic structure with precipitates rich in copper in the interdendritic areas. The authors stated in the summary that the electron beam welded joints were characterised by hardness in the weld area similar to that typical of TIG-welded joints or laser beam welded joints. However, smaller dimensions of the electron beam weld translated into smaller structural changes and, consequently, the lower reduction of material properties.

The authors (Olshanskaya T.V. et al.) from the Perm National Research Polytechnic University [11] performed research concerning the EBW technology involving the debunching of the beam and assessed the applicability of the dynamic electron beam positioning when welding aluminium alloy AlMg6. The beam was debunched into three (sub) beams using oscillation. The aforesaid method is referred to as multi-beam welding. The investigation of the effect of the debunched beam on the geometric characteristic of welds necessitated the performance of a series of experiments with the three-level planning matrix. The tests resulted in the identification of the correlation between depth, width as well as shape and penetration depth coefficients and the primary welding process parameters in relation to electron beam current, welding rate, beam exposure time at every spot and distances between individual beams. It was found that the obtainment of imperfection-free electron beam welds made of aluminium AlMg6 using the debunched beam required the conical shape of the weld with the rounded root. The EBW method involving the use of the debunched beam (multiple-beam welding) reduced material penetrability (by the beam) in comparison with that obtainable using the single electron beam process. The greatest effect on the weld depth was associated with the time of electron beam effect on each of gasodynamic channels formed during the test (during the so-called key-hole welding). The authors found that the obtainment of the maximum depth of penetration necessitated the significantly longer time of electron beam effect in the second gasodynamic channel than that in the first one. It was also observed that in increase in beam current was accompanied by increased penetrability, yet also by the reduced number of possible debunching.

However, the aforesaid situation decreased the number of possible debunching patterns enabling the obtainment of imperfection-free welds.

In one of the chapters of publication entitled Thermomechanical Industrial Processes: Modelling and Numerical Simulation [12] the authors describe FEM-based simulations of phenomena taking place during the electron beam welding of aluminium alloys of series 6061. The researchers observed that the rapid heating of the material to the melting point (by the electron beam) followed by very fast cooling triggered phenomena (in the material) significantly different to those occurring during other technological processes. It was ascertained that the modelling of the weld necessitated the identification of material properties at high temperature. Data from stress-strain curves (already published) did not include short times of microstructure formation during electron beam welding, which significantly affected results obtained in the tests. In their study, the authors proposed a phenomenological model of estimating hard and soft phases as well as corresponding mechanical properties. The experimentally observed stress-strain curves were successfully modelled in actual tests.

Article [13] by another team of Russian researchers (A.P. Sliva et al.) presents results of tests concerning the effect of electron beam oscillation on the geometry of joints made of aluminium alloys. It was demonstrated that the use of EBW with longitudinal oscillation combined with the appropriate frequency and amplitude of oscillation led to the generation of "lifting" force. The aforesaid force affected the weld pool metal, enabling the uninterrupted outflow of the metal from the weld root. The maximum liquid metal "lift" was observed in relation to a frequency of 35 Hz and an amplitude of 1 mm (for 12 mm thick aluminium alloys and a welding rate of 1500 mm/min). The above-presented effect could be used with EBW materials characterised by large thickness and uniform penetration, making it possible to prevent the formation of the welding imperfection typical of the EBW process, i.e. non-uniform and repeatable excess weld metal in the root. Depending on the thickness of joints subjected to welding, it was necessary to appropriately adjust frequency so that resultant force could compensate gravity. In terms of the electron beam welding of the 12 mm thick AlMg3 alloy, the highest quality of joints was observed in relation frequency restricted within the range of 90 Hz do 110 Hz.

A Japanese team led by Fujii Hidetoshi from Osaka University [14] performed research concerning the formation of porosity during the electron beam welding (EBW) process. The electron beam welding and TIG welding of aluminium alloys were performed both in normal gravity and microgravity environments. The authors proposed a new explanation concerning the mechanism responsible for the formation of porosity (simultaneously pointing to the common opinion that the primary factor responsible for porosity formation in aluminium alloys was hydrogen). The test results led to the conclusion that porosity was formed as a result of a reaction taking place between molten aluminium and Al_2O_3, leading to the formation of Al_2O. The observations made during the tests were the following:

- Porosity was formed only under vacuum during electron beam welding.
- Porosity was only located in the upper part, whereas hydrogen-induced porosity was located widely in the upper half. The above-named observation implied that the porosity was the result of a chemical reaction taking place at the highest temperature and not because of the reduced content of dissolved substance.
- Porosity (number of pores) was significantly reduced under microgravity conditions (during EBW), yet it increased during TIG welding when the process was shielded by gas containing hydrogen.
- Porosity (number of pores) increased along with the increased thickness of the oxide layer.

The comparison concerning the possibility of joining aluminium alloys using the electron beam welding and friction stir welding methods was also the subject of research performed by a Polish team composed of, among others, researchers from the Łukasiewicz Research Network – Upper Silesian Institute of Technology. Article [15] presents results concerning the joining of alloy EN AW-6082 T6. The FSW process was performed using a linear welding rate of 355 mm/min and a tool rotation rate of 710 rpm. In turn, the EBW process was performed using accelerating voltage U = 120 kV, beam current I = 18.7 mA and welding rate v = 1600 mm/min. The parameters used during smoothing melting included U = 80 kV, I = 17 mA and v = 700 mm/min. The test joints were subjected to complex microstructural tests (involving the use of light microscopy (LM), scanning electron microscopy (SEM) and transmission electron microscopy (TEM)), tests of mechanical properties (tensile tests and hardness measurements) as well as tests concerning the topography of cracks after the tensile test. The test results revealed that the mechanical properties of the EBW joints were reduced by 23 % in comparison with those of the base material. In turn, the mechanical properties of the FSW joints were reduced by 38 % in comparison with those of the base material. It was also possible to observe the reduction of elongation. In relation to the FSW joints, elongation amounted to 7.2 %, whereas in relation to the EBW joint, elongation amounted to 2.7 %. In addition, in terms of the EBW joints it was possible to observe the evaporation of magnesium from the weld during the welding process. In turn, in the FSW joints it was possible to observe the dissolution of Mg2Si particles (responsible for the hardening of the material during heat treatment) to state T6.

A Chinese team of researchers [16] (Xiaohong Zhan et al.) performed tests involving the making of joints using laser beam welding (LBW) and electron beam welding (EBW). The LBW joints were made using a laser power of 2.3 kW and a welding rate of 2500 mm/min, whereas the EBW joints were made using a power of 0.9 kW, an accelerating voltage of 60 kV and a welding rate of 1000 mm/min. The joints were made of 3 mm thick aluminium sheets (grade 5A06). The cross-sectional area of the weld made using the LBW process amounted to 4.34 mm^2, whereas the cross-sectional area of the weld made using the EBW process amounted to 2.6 mm^2. As can be seen, the cross-sectional area of the weld made using the EBW method constituted 59.91 % of cross-sectional area of the weld made using the LBW process. The weld made using the LBW method contained significant porosity, as opposed to the weld made using the EBW method. In addition, the weld made using the LBW method was characterised by a greater grain size than that observed in the weld made using the EBW method. Also, the mean hardness of the weld made using the LBW method was lower than that identified in the weld made using the EBW method. The tensile strength of the base material amounted to 377.92 MPa. The tensile strength values of the LBW and EBW-made welds amounted to 221.41 MPa and 289.41 MPa respectively. According to the authors, the quality of the EBW joints was higher than that of the LBW joints.

The overview of reference publications discussed in the previous part of the article led to the conclusion that the electron beam welding of aluminium alloys was preferable as it enabled the obtainment of the highest quality of welded joints. Because of high energy density, the possibility of controlling beam focus and oscillation as well as the due to the possible debunching of the beam, the method enabled the control of process linear energy and weld shape ensuring the satisfaction of quality-related criteria for welds made of most aluminium alloys usable in welding processes. In addition, the performance of the process under vacuum translated into the highest possible metallurgical purity of the former.

However, it should be noted that the EBW process is not without disadvantages. Because of the entirely different nature of the heat source and specific process conditions, the phenomena taking place when welding by means of the EBW method are different from those accompanying other metal joining process. For this reason, mechanisms responsible for the formation to porosity, post-weld stresses and strains as well as phenomena or welding imperfections characteristic of the method (e.g. "intermittent" weld root or the evaporation of some chemical elements constituting the weld) should be particularly taken into account when designing welded joints made of aluminium alloys and selecting an appropriate alloy grade.

3. Tests and results

All the tests discussed in the remainder of the article were performed at Łukasiewicz Research Network – Upper-Silesian Institute of Technology.

The research-related tests included the following tests and activities:

- making of test joints using previously determined welding parameters,
- visual tests (VT),
- macro and microscopic metallographic tests,
- tensile tests,
- bend tests,
- hardness measurements.

The welding of test joints was performed using an Xw150:30/756 electron beam welding and surface processing machine (Cambridge Vacuum Engineering). The macro and microscopic tests were performed in accordance with the requirements of the PN-EN ISO 17639: 2013-12 standard [17]. Microscopic observations were performed using an Eclipse MA200 microscope (Nikon). The assessment of welding imperfections (if any) was performed in accordance with the requirements specified in the PN-EN ISO 13919-2:2021-07 standard [18]. The tensile tests were performed in accordance with the requirements of the PN-EN

Table 1. Chemical compositions of the materials used in the tests

Alloy	Si		Fe		Cu	Mn	Mg		Cr	Zn	Ti	Other	Al
	Min.	Max.	Min.	Max.	Max.	Max.	Min.	Max.	Max.	Max.	Max.	Max.	
6060	0.30	0.60	0.10	0.30	0.10	0.10	0.35	0.60	0.05	0.15	0.10	0.15	bal.
6061	0.40	0.80	0.00	0.70	0.40	0.15	0.80	1.20	0.35	0.35	0.25	0.15	bal.
1A	1.00		0.00		0.60	0.60	0.70		0.25	0.00	0.02	-	bal.
1B	1.00		0.00		0.80	0.60	0.70		0.25	0.00	0.02	-	bal.
2A	1.20		0.00		0.80	0.60	0.80		0.25	0.00	0.02	-	bal.
2B	1.20		0.00		1.00	0.60	0.80		0.25	0.00	0.02	-	bal.
2C	1.20		0.00		0.80	0.60	0.80		0.25	0.40	0.02	-	bal.
3A	1.20		0.00		1.20	0.60	0.80		0.40	0.00	0.02	-	bal.
3B	1.20		0.00		1.40	0.60	0.80		0.40	0.00	0.02	-	bal.

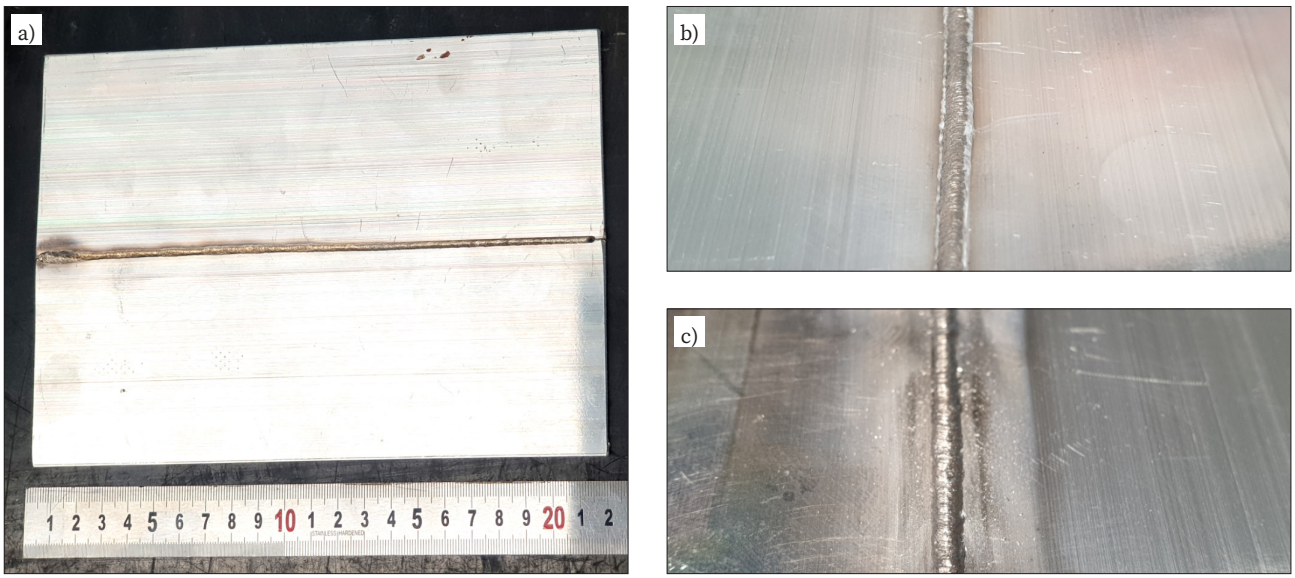

Fig. 1. Joint made of alloy grade 6060: a) main view, b) weld face and c) weld root

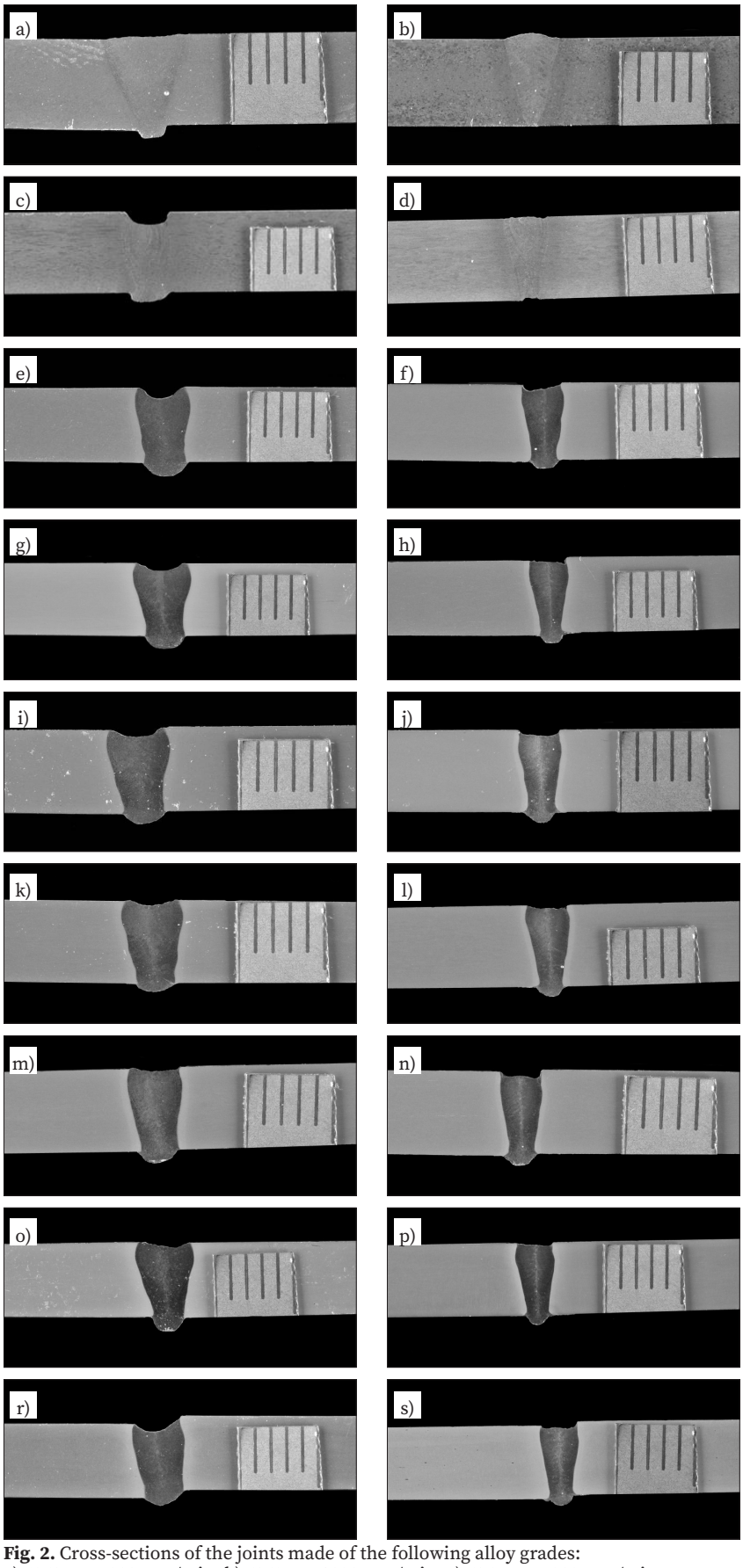

Fig. 2. Cross-sections of the joints made of the following alloy grades: a) 6060, v = 1000 mm/min, b) 6060, v = 2000 mm/min, c) 6061, v = 1000 mm/min, d) 6061, v = 2000 mm/min, e) 1A, v = 1000 mm/min, f) 1A, v = 2000 mm/min, g) 1B, v = 1000 mm/min, h) 1B, v = 2000 mm/min, i) 2A, v = 1000 mm/min, j) 2A, v = 2000 mm/min, k) 2B, v = 1000 mm/min, l) 2B, v = 2000 mm/min, m) 2C, v = 1000 mm/min, n) 2C, v = 2000 mm/min, o) 3A, v = 1000 mm/min, p) 3A, v = 2000 mm/min, r) 3B, v = 1000 mm/min, s) 3B, v = 2000 mm/min

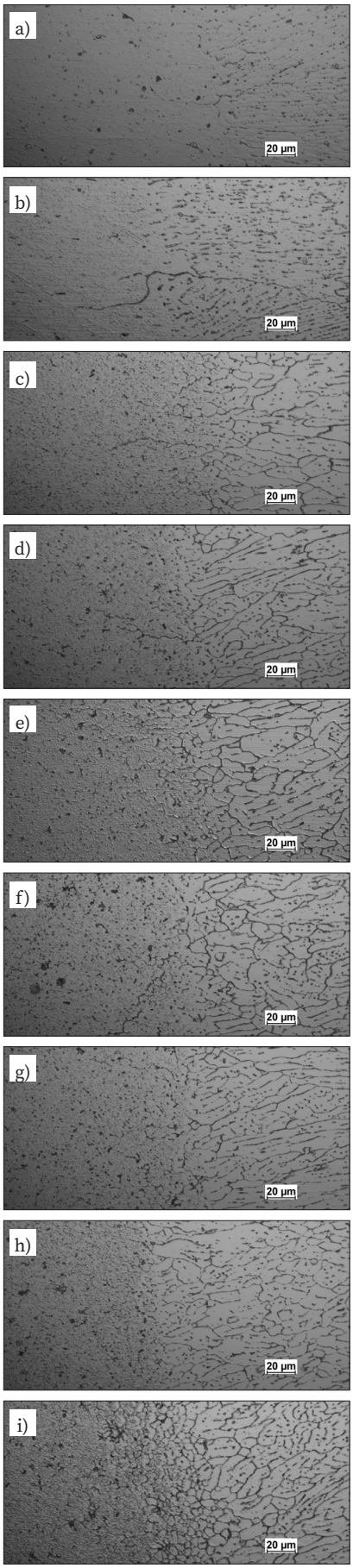

Fig. 3. Microstructures of the HAZ in the joints made of alloy grades: a) Al6060, b) Al6061, c) 1A, d) 1B, e) 2A, f) 2B, g) 2C, h) 3A, i) 3B

ISO 4136:2013-05 standard [19], using a C45.105E testing machine (MTS Criterion). The bend tests were performed in accordance with the requirements specified in the PN-EN ISO 5173:2010 standard Destructive tests on welds in metallic materials. Bend tests. [20] The tests involved the use of a dedicated testing machine (developed by Łukasiewicz – GIT) used for bend tests and involving the use of a roller. The hardness measurements were performed in accordance with the requirements specified in the PN-EN ISO 22826:2021-08 standard Destructive testing of welds in metals — Test of hardness of narrow joints welded by laser and electron beam (hardness tests by Vickers and Knoop method) [21], using a KB50BYZ-FA hardness tester.

The welding process parameters were the following:

- accelerating voltage: 80 kV,
- beam current restricted within the range of 28.5 mA to 25 mA (decreasing along the joint length) in relation to a travel rate (welding rate) of 1000 mm/min,
- beam current restricted within the range of 37 mA to 34 mA (decreasing along the joint length) in relation to a travel rate (welding rate) of 2000 mm/min,
- cathode heater current: 21 A,
- focal length: 470 mm,
- focusing current: 530 mA,
- oscillation shape: circular,
- oscillation frequency: 100 Hz,
- oscillation amplitude: 1 mm.

Exemplary joints (made of alloy grade 6060) are presented in Figure 1.

The cross-sections of all the joints are presented in Figure 2. Except for the joints made of aluminium alloy grade 6061, i.e. 1A and 3B, represented quality level B. In addition, all the joints represented quality level C. The assessment of welding imperfections was performed in accordance with the recommendations contained in the PN-EN ISO 13919-2:2021-07 standard [18].

After the macroscopic tests, the joints were observed using scanning electron microscopy. To reveal their structure, the joints were etched in a mix composed of 65 % H_2O, 20 % of concentrated nitric acid, 20 % of concentrated hydrochloric acid and 5 % of hydrofluoric acid. The microstructures revealed in the tests did not differ significantly. Figure 3 presents the HAZ microstructures in all of the joints welded at a rate of 2000 mm/min.

In the weld material of each joint it was possible to observe the clearly visible fusion line as well as columnar and equiaxial crystallites. Most of the weld microstructures contained easily visible intercrystalline spaces. The base material contained clearly visible precipitates of varied dispersion, the concentration of which changed in relation to specific alloys; the highest concentration was observed in the alloys of series 3 (particularly 3B), whereas the lowest concentration was observed in alloy Al6060.

The subsequent stage involved the performance of hardness measurements. Figures 4–12 present hardness distribution in the cross-sections of the test joints.

In cases of the joints made of experimental alloy grades it was possible to observe a reverse tendency, i.e. the HAZ and the weld of the joints were characterised by an increase in hardness (particularly in the HAZ). In terms of alloys 1A, 1B, 2A, 2B and 2C (Figures 8 through 12) it was possible to observe a welding-triggered increase in hardness from approximately 60 HV in the base material to approximately 90 HV (i.e. by 50 %) in the HAZ and a decrease to approximately 80 HV (i.e. by 11 %) in the weld. In turn, the joints made of alloys 3A and 3B (Figures 13 and 14) were

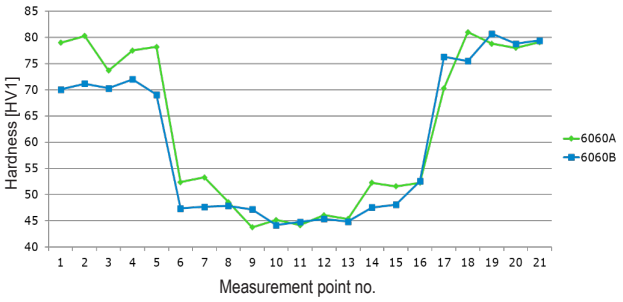

Fig. 4. Cross-sectional hardness distribution in the welded joint made of aluminium alloy grade 6060

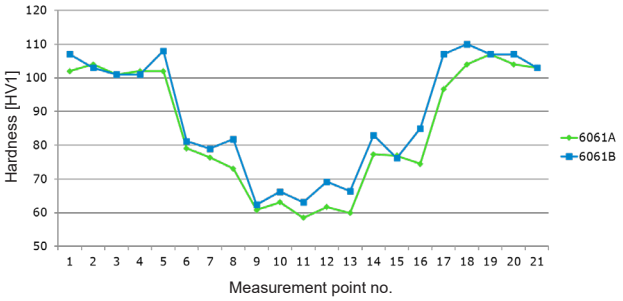

Fig. 5. Cross-sectional hardness distribution in the welded joint made of aluminium alloy grade 6061

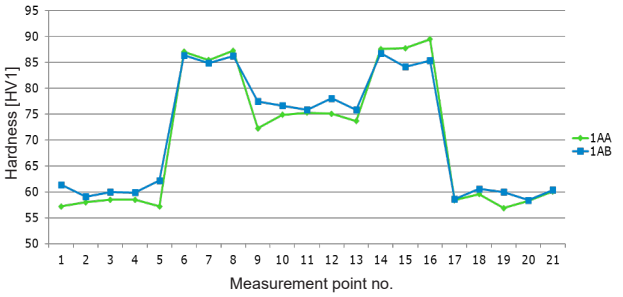

Fig. 6. Cross-sectional hardness distribution in the welded joint made of aluminium alloy grade 1A

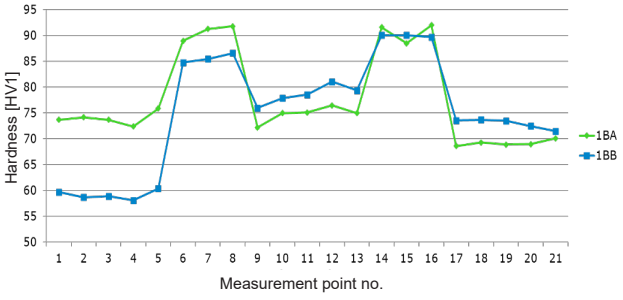

Fig. 7. Cross-sectional hardness distribution in the welded joint made of aluminium alloy grade 1B

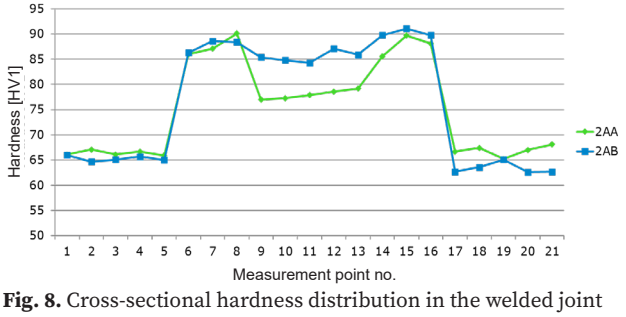

Fig. 8. Cross-sectional hardness distribution in the welded joint made of aluminium alloy grade 2A

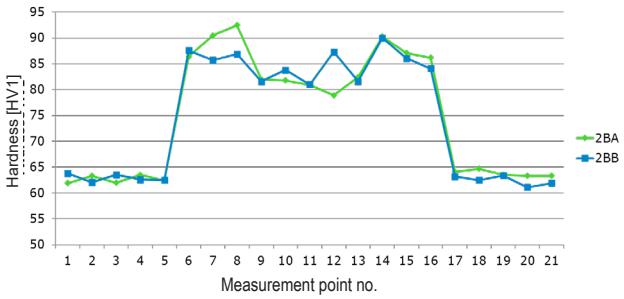

Fig. 9. Cross-sectional hardness distribution in the welded joint made of aluminium alloy grade 2B

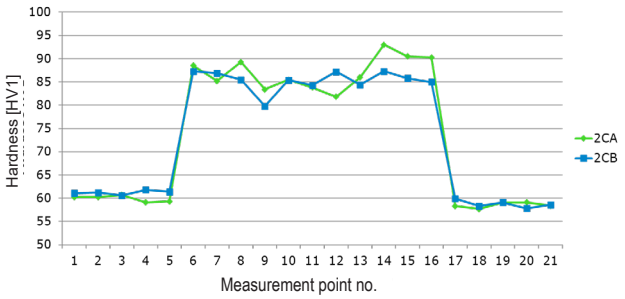

Fig. 10. Cross-sectional hardness distribution in the welded joint made of aluminium alloy grade 2C

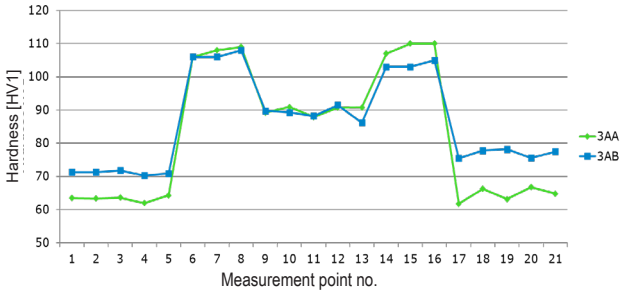

Fig. 11. Cross-sectional hardness distribution in the welded joint made of aluminium alloy grade 3A

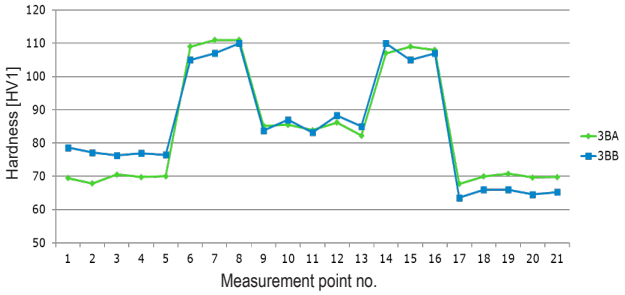

Fig. 12. Cross-sectional hardness distribution in the welded joint made of aluminium alloy grade 3B

Table 2. Tensile test results concerning the joints made of the commercial aluminium alloys

Alloy symbol	Specimen number	Welding rate [mm/min]	Tensile strength $R_{m,}$ [MPa]	Acceptance criterion $R_{m\,min}$ [MPa]	Rupture location
AW6060 T6	1.1	1000	165.9	110.5	in the weld
	1.2		165.3		in the weld
	2.1	2000	162.2		in the weld
	2.2		164.8		in the weld
AW 6061	1.1	1000	230.3	188.5	in the weld
	1.2		225.0		in the weld
	2.1	2000	230.1		in the weld
	2.2		226.1		in the weld

characterised by an increase in hardness from approximately 70 HV in the base material to approximately 110 HV (i.e. by 57 %) in the HAZ and a decrease to 85 HV (by 22 %) in the weld.

The subsequent stage involved the performance of transverse tensile tests of all the joints; each joint was subjected to two tests. The test results concerning the joints made of alloy grades 6060 and 6061 are presented in Table 2, whereas the test results concerning the joints made of experimental alloys are presented in Table 3. The determination of the acceptance criterion for the specimens made of experimental alloys necessitated the performance of tensile tests involving each material. The acceptance criterion presented in Tables 2 and 3 constituted 65 % of the measured base material tensile strength.

All the joints subjected to the tensile tests satisfied the required criterion, i.e. R_m min. > 65 % R_m of the base material. In addition, all the specimens (except for the specimen made of alloy 2C using a welding rate of 2000 mm/min as well as the specimens made of alloy grades 6060 and 6061) ruptured in the base material. It was also observed that an increase in the content of copper was accompanied by an increase in the strength of the welded joints from 160 MPa (alloy 6060) up to as many as approximately 280 MPa (alloy 3B). The increased hardness in the HAZ and in the weld as well as the fact that most of the specimens made of the experimental alloys ruptured in the base material indicated the electron beam welding-triggered hardening of the alloy. The reason for the above-presented phenomenon should be the subject of further research using more advance X-ray techniques and electron microscopy.

The final stage involved the performance of bend tests (including all the welded joints). Before the tests, excessively large reinforcements (excess weld metal) on the weld face or excess weld metal on the root (if any) were ground off. Afterwards, each joint was subjected to two face bend tests and two root bend tests. The joint made of alloy 6060 was bent using a bending pin having a diameter of 15 mm. The joints made of alloy grades 1A and 1B were bent using a bending pin having a diameter of 20 mm. The joints made of alloy grades 6061, 2A, 2B and 2C were bent using a bending pin having a diameter of 25 mm. The joint

Table 3. Tensile test results concerning the joints made of the experimental aluminium alloys

Alloy symbol	Specimen number	Welding rate [mm/min]	Tensile strength R_m [MPa]	Acceptance criterion $R_{m\,min}$ [MPa]	Rupture location
1A	1A.1/1	1000	225.9	151.5	outside the weld
	1A.1/2		211.6		outside the weld
	1A.2/1	2000	225.2		outside the weld
	1A.2/2		221.4		outside the weld
1B	1B.1/1	1000	238.8	156.0	outside the weld
	1B.1/2		231.6		outside the weld
	1B.2/1	2000	213.6		outside the weld
	1B.2/2		213.0		outside the weld
2A	2A.1/1	1000	247.8	163.8	outside the weld
	2A.1/2		235.4		outside the weld
	2A.2/1	2000	231.6		outside the weld
	2A.2/2		228.8		outside the weld
2B	2B.1/1	1000	236.4	169.0	outside the weld
	2B.1/2		238.4		outside the weld
	2B.2/1	2000	234.8		outside the weld
	2B.2/2		236.4		outside the weld
2C	2C.1/1	1000	222.0	163.2	outside the weld
	2C.1/2		221.0		outside the weld
	2C.2/1	2000	220.7		w SWC
	2C.2/2		224.0		w SWC
3A	3A.1/1	1000	244.1	197.0	outside the weld
	3A.1/2		249.1		outside the weld
	3A.2/1	2000	258.9		outside the weld
	3A.2/2		261.2		outside the weld
3B	3B.1/1	1000	245.2	180.7	outside the weld
	3B.1/2		240.0		outside the weld
	3B.2/1	2000	274.3		outside the weld
	3B.2/2		289.7		outside the weld

made of alloy 3A was bent using a bending pin having a diameter of 30 mm. The joint made of alloy 3B was bent using a bending pin having a diameter of 40 mm. The diameters of the bending pins were selected in accordance with the requirements specified in the PN-EN ISO 5173:2010 standard Destructive tests on welds in metallic materials. Bend tests [20] and identified on the basis of the results of previously performed tensile tests involving base materials. The bend angle amounted to 180°. The joint made of alloy grade 1B using a welding rate of 1000 mm/min, subjected to the root bend test contained a crack having a length of 15 mm. It was possible to notice 5 mm long cracks in the specimens made of alloy grades 2A and 2C (1 piece each) using a welding rate of 1000 mm/min and subjected to bending on the weld root side. A crack across the entire width was observed in the specimens made of alloy grades 2C, 3A and 3B (1 piece each) using a welding rate of 2000 mm/min and subjected to bending on the weld face side. It was also possible to notice 10 mm long cracks in the specimens made of alloy grade 3A using a welding rate of 1000 mm/min and in the specimens made of alloy grade 3B using a welding rate of 2000 mm/min and subjected to bending on the weld root side. The remaining specimens did not contain any cracks or discontinuities.

4. Conclusions

The visual tests and macroscopic metallographic tests revealed that most of the joints represented quality level B (except for the joints made of aluminium alloy grade 6061, i.e. 1A and 3B, representing quality level C). The assessment of the joints was performed following the requirements specified in the PN-EN ISO 13919-2:2021-07 standard.

All the joints subjected to the tensile tests satisfied the required criterion, i.e. $R_{m\,min.} > 65\ \%\ R_m$ of the base material.

In addition, all the specimens (except for the specimen made of alloy 2C using a welding rate of 2000 mm/min as well as the specimens made of alloy grades 6060 and 6061) ruptured in the base material.

It was observed that an increase in the content of copper was accompanied by an increase in the strength of the welded joints from 160 MPa (alloy 6060) up to as many as approximately 280 MPa (alloy 3B)

The analysis of hardness measurement results concerning alloys 1A, 1B, 2A, 2B and 2C revealed a welding-triggered increase in hardness from approximately 60 HV in the base material (BM) to approximately 90 HV (i.e. by 50 %) in the heat affected zone (HAZ) and a decrease to approximately 80 HV (i.e. by 11 %) in the weld. In turn, the joints made of alloys 3A and 3B were characterised by an increase in hardness from approximately 70 HV in the BM to approximately 110 HV (i.e. by 57 %) in the HAZ and a decrease to 85 HV (by 22 %) in the weld.

The increased hardness identified in the HAZ and in the weld as well as the fact that most of the specimens made of the experimental alloys (except for the joint made of alloy 2C using a welding rate of 2000 mm/min) ruptured in the base material indicated the electron beam welding-triggered hardening of the alloy. The reason for the above-presented phenomenon should be the subject of further research using more advance X-ray techniques and electron microscopy

Because of the post-bend test presence of unacceptable cracks, the joints made of alloy grades 1B, 2A, 2C and 3A using a welding rate of 1000 mm/min as well as the joints made of alloy grades 2C, 3A and 3B using a welding rate of 2000 mm/min failed to meet the requirements of the PN-EN ISO 5173:2010.

The microscopic metallographic tests did not reveal the presence of unacceptable welding imperfections (e.g. microcracks) in the joints.

Article submitted to the 28th Scientific and Technical National Welding Conference "Progress, innovations and quality requirements of welding processes"(Międzyzdroje, 21-23.05.2024 r.)

REFERENCES

[1] Dobrzański L.A.: Materiały inżynierskie i projektowanie materiałowe. Podstawy nauki o materiałach i metaloznawstwo. Wydawnictwo Naukowo-Techniczne, Warszawa 2006.
[2] Pilarczyk J., Węglowski M.S.: Spawanie wiązką elektronów. Welding Technology Review, 2015, vol. 87, no. 10, pp. 124-129.
[3] Węglowski M.S., Jachym R., Krasnowski K., Kwieciński K., Pikuła J., Śliwiński P.: Electron Beam Melting of Thermally Sprayed Layers – Overview. Biuletyn Instytutu Spawalnictwa, 2021, vol. 65, no. 3, pp. 7–19.
[4] Maajid Ali, Vadali S.K., Maury D.K. Saha, Tanmay K.: Electron beam welding of aluminium components. Indian Vacuum Society, India 2015.
[5] Sobih M., Elseddig Z.: Electron Beam Welding of Aluminum Alloys. Encyclopedia of Aluminum and Its Alloys. 2019. CRC Press. ISBN 9781351045636.
[6] Lipińska M., Pixner F., Szachogłuchowicz I., Mittermayr F., Grengg C., Enzinger N., Lewandowska M.: Application of electron beam welding technique for joining coarse-grained and ultrafine-grained plates from Al-Mg-Si alloy. Journal of Manufacturing Processes 2023, 104, pp. 28–43.
[7] Soo-sung Kim i in.: Development of electron beam welding technology using AA6061-T6 aluminium alloy for nuclear fuel plate assembly. Proceedings of the 2013 21st International Conference on Nuclear Engineering ICONE21.
[8] Alexopoulos N.D., Examilioti T.N., Stergiou V., Kourkoulis S.: Tensile mechanical performance of electron-beam welded joints from aluminum alloy (Al-Mg-Si) 6156. Procedia Structural Integrity. 2016, no. 2, pp. 3539-3545.
[9] Hayat F.: Electron beam welding of 7075 aluminum alloy: Microstructure and fracture properties. Engineering Science and Technology, an International Journal, vol. 34, 2022.
[10] Wanjara P., Brochu M.: Characterization of electron beam welded AA2024. Vacuum, 2010, vol. 85, no. 2, pp. 268–282.
[11] Olshanskaya T.V., Salomatova E.S., Belenkiy V.Y., Trushnikov D.N., Permaykov G.L: Electron beam welding of aluminum alloy AlMg6 with a dynamically positioned electron beam. Int J Adv Manuf Technol. 2017, vol. 89, pp. 3439–3450.
[12] Nelias D. i in.: Thermomechanical Industrial Processes: Modeling and Numerical Simulation. Chapter 2: Laser and Electron Beam Welding of 6xxx Series Aluminum Alloys – On Some Thermal, Mechanical and Metallurgical Aspects, (ed.) Jean-Michel Bergheau. ISTE Ltd 2014. Published by ISTE Ltd and John Wiley & Sons, Inc.
[13] Sliva A.P., Dragunov V.K., Terentyev E.V., Goncharov A.L.: EBW of aluminium alloys with application of electron beam oscillation. OP Conf. Series: Journal of Physics: Conf. Series. 2018, 1089.
[14] Fujii H., Umakoshi H., Aoki Y., Nogi K.: Bubble formation in aluminium alloy during electron beam welding. Journal of Materials Processing Technology, vol. 155–156, 2004, pp. 252–1255.
[15] Noga P., Skrzekut T., Wędrychowicz M., Węglowski M.S., Węglowska A.: Research of Friction Stir Welding (FSW) and Electron Beam Welding (EBW) Process for 6082-T6 Aluminum Alloy. Materials, 2023, vol. 16, no. 14, 4937.
[16] Xiaohong Zhan et al.: A comparative study on laser beam and electron beam welding of 5A06 aluminum alloy. Mater. Res. Express, 2019, vol. 6, no. 5, 056563.
[17] PN-EN ISO 17639: 2013-12 Badania niszczące spawanych złączy metali – Badania makroskopowe i mikroskopowe złączy spawanych.
[18] PN-EN ISO 13919-2:2021-07 Złącza spawane wiązką elektronów i wiązką promieniowania laserowego. Wymagania i zalecenia do określania poziomów jakości według niezgodności spawalniczych. Część 2: Aluminium, magnez i ich stopy i oraz czysta miedź.
[19] PN-EN ISO 4136:2013-05 Badania niszczące złączy spawanych metali. Próba rozciągania próbek poprzecznych.
[20] PN-EN ISO 5173:2010 Badania niszczące spoin w materiałach metalowych – Badanie na zginanie.
[21] PN-EN ISO 22826:2021-08 Badania niszczące spoin w metalach. Badanie twardości wąskich złączy spawanych wiązką laserową i elektronową (badania twardości sposobem Vickersa i Knoopa).